Emergence of entanglement out of a noisy environment: The case of microcavity polaritons

S. PORTOLAN[1,2(a)], O. DI STEFANO[3], S. SAVASTA[3] and V. SAVONA[1]

[1] *Institute of Theoretical Physics, Ecole Polytechnique Fédérale de Lausanne EPFL - CH-1015 Lausanne, Switzerland*
[2] *CEA/CNRS/UJF Joint Team "Nanophysics and Semiconductors", Institut Néel, CNRS*
BP 166, 25 rue des Martyrs, 38042 Grenoble Cedex 9, France, EU
[3] *Dipartimento di Fisica della Materia e Ingegneria Elettronica, Università di Messina*
Salita Sperone 31, I-98166 Messina, Italy, EU

Abstract – We show theoretically that polariton pairs with a high degree of polarization entanglement can be produced through parametric scattering. We demonstrate that entanglement can emerge in coincidence experiments, even at low excitation densities where the dynamics is dominated by incoherent photoluminescence. Our analysis is based on a microscopic quantum statistical approach that treats coherent and incoherent processes on an equal footing, thus allowing for a quantitative assessment of the amount of entanglement under realistic experimental conditions. This result puts forward the robustness of pair correlations in solid-state devices, even when noise dominates one-body properties. In particular, we propose an operational method to measure the entanglement of formation, out of a dominant time-dependent noise background, without any need for post-processing. Our study provides a suggestive perspective towards hybrid all-optical quantum devices where quantum information can be efficiently generated and controlled within the same structure.

Introduction. – The concept of *entanglement* has played a crucial role in the development of quantum physics. It can be described as the correlation between distinct subsystems which cannot be reproduced by any classical theory (*i.e. quantum correlation*). It has gained renewed interest mainly because of the crucial role that such concept plays in quantum information/computation (QIC) [1], as a precious resource enabling to perform tasks that are either impossible or very inefficient in the classical realm [2]. Scalable solid-state devices will make use of local electronic states to store quantum correlations [3]. Polaritons [4], on the other hand, as hybrid states of electronic excitations and light, are the most promising solution for generation and control of quantum correlations over long range [5]. In particular, thanks to the Coulomb interaction acting on the electronic part of the polariton state, resonantly generated pump polaritons scatter into pairs of *signal* and *idler* polaritons, in a way

that fulfills total energy and momentum conservation. The generated polariton pairs can be in an entangled state [6,7]. In this case the outcome of a polariton parametric scattering is an *entangled state of a hybrid quasiparticle, half light and half electronic excitation, of the semiconductor* —the polariton pair— contrarily to parametric downconversion in a nonlinear crystal [6], where only the outgoing photons are entangled. Here, the emitted photons serve merely as a probe of the internal degree of entanglement. Thanks to their photon component, polaritons can sustain quantum correlations over mesoscopic distances inside the semiconductor. This is why they bear a unique potential as a controllable embedded mechanism to generate quantum information in a device and transfer it to localized qubits (*e.g.*, spin qubits) over distances of microns [5]. The peculiar energy momentum dispersion of microcavity polaritons has the advantage of allowing several configurations of parametric scattering, that can be easily selected by setting the frequency and angle of both the pump and the

---

(a)E-mail: stefano.portolan@grenoble.cnrs.fr

detected beams [8,9]. In order to address entanglement in quantum systems [10,11], the preferred experimental situation is the few-particle regime in which the emitted particles can be detected individually [12]. In a real system, environment always act as an uncontrollable and unavoidable continuous perturbation producing decoherence and noise. Even if polariton experiments are performed at temperatures of few kelvins [13], polaritons created resonantly by the pump can scatter, by emission or absorption of acoustic phonons, into other states, acquiring random phase relations. These polaritons form an incoherent background (*i.e.* noise), responsible of *pump-induced* photoluminescence (PL), which competes with coherent photoemission generated by parametric scattering, as evidenced by experiments [9]. As a consequence, noise represents a fundamental limitation, as it tends to lower the degree of nonclassical correlation or even completely wash it out [13,14]. Hence understanding the impact of noise on quantum correlations in semiconductor devices, where the electronic system cannot be easily isolated from its environment, is crucial.

In this letter, we present a microscopic study of the influence of time-dependent noise on the polarization entanglement of polaritons generated in parametric PL. Our treatment accounts for realistic features such as detectors noise background, detection windows, dark-counting etc., needed [15] in order to seek and limit all the unwanted detrimental contributions. We show how a tomographic reconstruction [16], based on two-times correlation functions, can provide a quantitative assessment of the level of entanglement produced under realistic experimental conditions. In particular, we give a ready-to-use realistic experimental configuration able to measure the Entanglement of Formation (EOF) [17,18], out of a dominant time-dependent noise background, without any need for post-processing [11].

Coherent and incoherent polariton dynamics. – Third-order nonlinear optical processes in quantum well excitons (with spin $\sigma = \pm 1$) can be described in terms of two distinct scattering channels: one involving only excitons (polaritons) with the same circular polarization (co-circular channel); and the other (counter-circular channel) due to the presence of both bound biexciton states and four-particle scattering states of zero angular momentum ($J = 0$) [19]. Bound biexciton-based entanglement generation schemes [10,20], producing entangled polaritons with opposite spin, need specific tunings for efficient generation, and are expected to carry additional decoherence and noise due to the scattering of biexcitons. Moreover, linearly polarized single-pump excitation cannot avoid the additional presence of the co-circular scattering channel which can lower polarization entanglement. The experimental set-up that we will choose to calculate the emergence of polariton spin entanglement is a two-pump scheme under pulsed excitation, involving the lower polariton branch only. The pumps (p_1 and p_2)
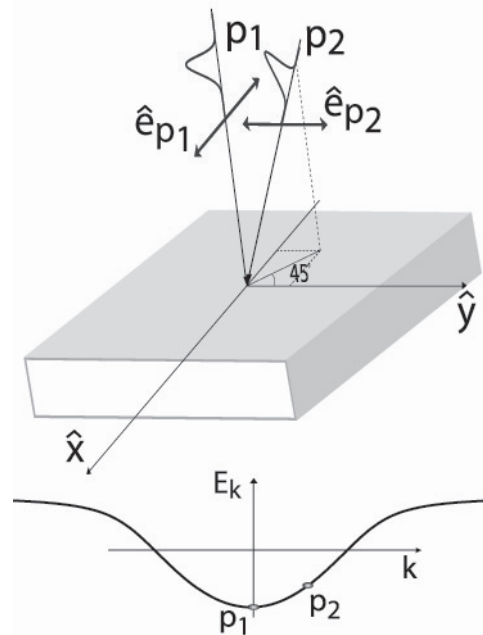

Fig. 1: Sketch of the proposed excitation geometry and of the lower polariton branch. The Gaussian pumps are linearly cross-polarized with zero time delay. The specific polarization configuration with $\theta = 0$, where θ is the angle between $\hat{e}_{p1}$ and the x-axis on the xy-plane, is depicted.

are chosen with incidence angles below the *magic angle* [9] so that single-pump parametric scattering is negligible. In this set-up, mixed-pump processes (signal at in-plane wave vector $\mathbf{k}$, idler at $\mathbf{k}_i = \mathbf{k}_1 + \mathbf{k}_2 - \mathbf{k}$) are allowed. We choose $\mathbf{k}_1 = (0., 0.)$, and $\mathbf{k}_2 = (0.9, 0.9)\,\mu\mathrm{m}^{-1}$. As signal-idler pair, we choose to study the two energy-degenerate modes at $\mathbf{k} \simeq (k_{1x}, k_{2y})$ and $\mathbf{k}_i \simeq (k_{2x}, k_{1y})$, as shown in fig. 1 and fig. 2. Of course a number of different two-pump schemes can also conveniently be adopted. For istance, from an experimental viewpoint, a two energy-degenerate pumps setting can be more valuable. Then possible choices for signal-idler pairs within the circle of available parametrically generated final states (see fig. 2) would suffer only a slightly unbalance being anyway close to the origin of the polariton dispersion curve. For all the numerical simulations we will consider the sample investigated in ref. [9]. In particular, we shall employ two pump beams linearly cross-polarized (then the angle θ will refer to the polarization of one of the two beams, see fig. 1). This configuration is such that the counter-circular scattering channel (both bound biexciton and scattering states) is suppressed owing to destructive interference, while co-circular polarized signal-idler beams are generated. In the absence of the noisy environment, polariton pairs would be cast in the pure triplet entangled state $|\psi_\parallel\rangle = |+, +\rangle - \exp(i4\theta)|-, -\rangle$.

The advantages of this configuration are manifold. First, detrimental processes for entanglement as the excitation-induced dephasing results to be largely suppressed [21].
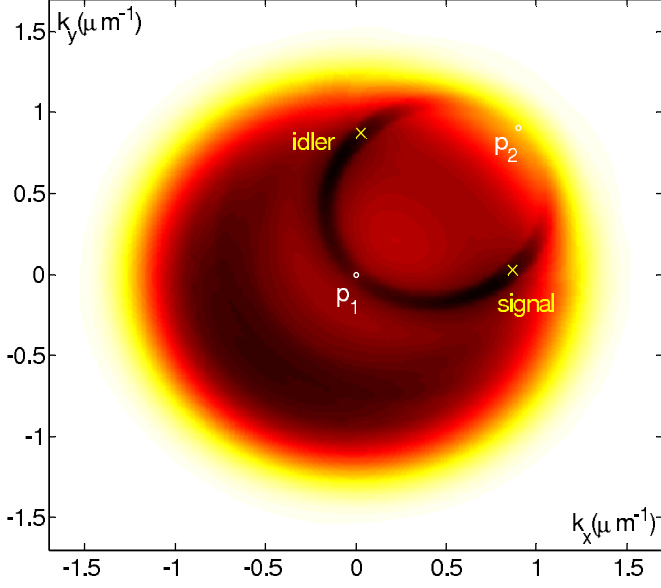
Fig. 2: (Color online) The simulated spectrally integrated polariton population in **k**-space. The parametric process builds up a circle passing through the two pumps (p_1 and p_2), signal and idler polariton states are represented by any two points on the circle connected by a line passing through its center. For illustration the pair of signal-idler polariton modes chosen for entanglement detection are depicted as yellow crosses. The disc-shape contribution centered at the origin is the incoherent population background produced by phonon scattering.

Spurious coherent processes, *e.g.* resonant Rayleigh scattering [22], are well separated in k-space from the signal and idler modes. In addition signal and idler close to the origin in **k**-space make negligible the longitudinal-transverse splitting of polaritons [23] (relevant at quite high in-plane wave vectors).

Following ref. [16] the tomographic reconstruction of the two-polariton density matrix is equivalent, in the $\sigma = \{+, -\}$ polarization basis, to the two-time coincidence

$$
\begin{aligned}
\rho_{\sigma\tilde{\sigma},\sigma'\tilde{\sigma}'} = &\frac{1}{\mathcal{N}} \int_{T_\mathrm{d}} \mathrm{d}t_1 \int_{T_\mathrm{d}} \mathrm{d}t_2 \langle \hat{P}_{\mathbf{k}\sigma}^{\dagger}(t_1) \hat{P}_{\mathbf{k}_i\tilde{\sigma}}^{\dagger}(t_2) \\
&\times \hat{P}_{\mathbf{k}_i\tilde{\sigma}'}(t_2) \hat{P}_{\mathbf{k}\sigma'}(t_1) \rangle,
\end{aligned}
\tag{1}
$$

where $\hat{P}_{\mathbf{k}\sigma}^{\dagger}$ ($\hat{P}_{\mathbf{k}_i\tilde{\sigma}}^{\dagger}$) creates a signal polariton at **k** (an idler polariton at $\mathbf{k}_i = \mathbf{k}_1 + \mathbf{k}_2 - \mathbf{k}$), $\mathcal{N}$ is a normalization constant and T_d the detector window. We choose a very wide time window $T_d = 120\,\mathrm{ps}$, allowing feasible experiments with standard photodetectors. In order to model the density matrix eq. (1), we employ the dynamics-controlled truncation scheme (DCTS), starting from the electron-hole Hamiltonian including two-body Coulomb interaction and radiation-matter coupling. In this approach nonlinear parametric processes within a third-order optical response are microscopically calculated. The main environment channel is acoustic phonon interaction via deformation potential coupling [15,24].

We use a DCTS-Langevin approach [15], with noise sources given by exciton-LA-phonon scattering and radiative decay (treated in the Born-Markov approximation). For mixed-pump processes with arbitrary polarization the Heisenberg-Langevin equations of motion read

$$
\begin{aligned}
\frac{\mathrm{d}}{\mathrm{d}t}\hat{P}_{\mathbf{k}\sigma} &= -i\tilde{\omega}_{\mathbf{k}}\hat{P}_{\mathbf{k}\sigma} - ig_{|\sigma_1+\sigma_2|}\hat{P}_{\mathbf{k}_i\sigma_i}^{\dagger}\mathcal{P}_{\mathbf{k}_1\sigma_1}\mathcal{P}_{\mathbf{k}_2\sigma_2} + \hat{\mathcal{F}}_{\hat{P}_{\mathbf{k}\sigma}} \\
\frac{\mathrm{d}}{\mathrm{d}t}\hat{P}_{\mathbf{k}_i\sigma_i}^{\dagger} &= i\tilde{\omega}_{\mathbf{k}_i}^{*}\hat{P}_{\mathbf{k}_i\sigma_i}^{\dagger} + ig_{|\sigma_1+\sigma_2|}\hat{P}_{\mathbf{k}\sigma}\mathcal{P}_{\mathbf{k}_1\sigma_1}^{*}\mathcal{P}_{\mathbf{k}_2\sigma_2}^{*} + \hat{\mathcal{F}}_{\hat{P}_{\mathbf{k}_i\sigma}^{\dagger}}.
\end{aligned}
\tag{2}
$$

In eq. (2) $\mathcal{P}_{\mathbf{k},\sigma}$ are the projections onto the circular basis σ of the coherent pump polariton fields. The explicit expression of the various terms entering the equations of motion (2) are

$$
\tilde{\omega}_{\mathbf{k}} = \omega_{\mathbf{k}} - i\Gamma_{\mathbf{k}}^{(\mathrm{tot})}/2 + \sum_{p=1,2} h_{\mathbf{k}}^{(p)} \left| \mathcal{P}_{\mathbf{k}_p}^{\pm} \right|^2,
\tag{3}
$$

$$
\begin{aligned}
h_{\mathbf{k}}^{(p)} = &\, X_{\mathbf{k}} \left[\frac{V}{n_{\mathrm{sat}}} X_{\mathbf{k}_p} \left(C_{\mathbf{k}_p} X_{\mathbf{k}} + X_{\mathbf{k}_p} C_{\mathbf{k}} \right) \right. \\
&\left. + 2V_{\mathrm{xx}} X_{\mathbf{k}_p} X_{\mathbf{k}_p} X_{\mathbf{k}} \right],
\end{aligned}
\tag{4}
$$

where X's and C's are the exciton and photon fractions in the lower polariton branch [15]. The complex polariton dispersion $\tilde{\omega}_{\mathbf{k}}$ includes the effects of relaxation and pump-induced renormalization (shifts $h_{\mathbf{k}}^{(p)}$), g is the nonlinear interaction term driving the mixed parametric processes [15]; summation over the repeated polarization indices σ_1 and σ_2 is assumed and the following selection rule holds: $\sigma_s + \sigma_i = \sigma_1 + \sigma_2$. $h_{\mathbf{k}}^{(p)}$ is the shift induced by the p-th pump due to the parametric process. The damping term $\Gamma_{\mathbf{k}}^{(\mathrm{tot})}$ results from a microscopic calculation including a thermal phonon bath whose details are given in ref. [15]. V_{xx} is the mean field while V is the phase-space filling interaction strengths [21,25]. In general, third-order contributions due to Coulomb interaction between excitons account for terms beyond mean field, including an effective reduction of the mean field interaction and an excitation-induced dephasing. It has been shown that both effects depend on the sum of the frequencies of the scattered polariton pairs [21]. For the frequency range here exploited, the excitation-induced dephasing is vanishingly small and can be safely neglected on the lower polariton branch [21]. On the contrary, the matrix elements of the ($J = 0$) counter-circular scattering channel is lower (about $1/3$) than that for the co-polarized scattering channel, but certainly not negligible [21]. However, in the pump polarization scheme that we propose, performing the polarization sum in eq. (2), it is easy to see that the counter-circular channel cancels out, as already pointed out. This feature is unique to the present scheme, while all previously adopted pump configurations suffer from the presence of both co- and counter-circular polarized scattering channels. Equation (2) is a system of two coupled equations for polariton operators, acting onto

the global system and environment state space, thanks to the two additive noise sources $\hat{\mathcal{F}}_{\hat{P}_{\mathbf{k}\sigma}}$, $\hat{\mathcal{F}}_{\hat{P}^{\dagger}_{\mathbf{k}_i\sigma}}$ [15,26][1].

Results. – Figure 2 shows a typical pattern of photoluminescence in **k**-space that we can simulate with our microscopic model. We can neatly distinguish the disc-shape contribution centered at the origin due to the incoherent population produced by phonon scattering from the parametric ring dynamically emerging from the noisy background. The two pumps employed are marked as p_1 and p_2. Parametrically generated signal and idler polariton states are represented by any two points on the circle connected by a line passing through its center. For illustration the pair of signal-idler polariton modes chosen for entanglement detection are depicted as yellow crosses. Early experiments in semiconductor microcavities [13,27] provided promising, though indirect, indications of polariton entanglement. In order to achieve a conclusive evidence of entanglement one has to produce its quantitative analysis and characterization, *i.e.* a *measure* of entanglement. Among the various measures proposed in the literature we shall use the *entanglement of formation* $E(\hat{\rho})$ [17,18] for which an explicit formula as a function of the density matrix exists[2]. It has a direct operational meaning as the minimum amount of information needed to *form* the entangled state under investigation out of uncorrelated ones (see footnote [2]). The complete characterization of a quantum state requires the knowledge of its density matrix. Even though its off-diagonal elements are not directly related to physical observables, the density matrix of a quantum system composed by two two-level particles can be reconstructed using the recently developed *quantum state tomography* [16], that has also been exploited in a bulk semiconductor [10]. It requires 16 two-photon coincidence measurements based on various polarization configurations [16]. Exploiting the Wick factorization [28,29] and the symmetries of the system, the density matrix elements are built up on the signal and idler occupation $N_{s/i\pm} \doteq \langle \hat{P}^{\dagger}_{s/i\pm}(\tau)\hat{P}_{s/i\pm}(\tau)\rangle$ ($\mathbf{k}=s,i$ mean the chosen signal, idler **k** vectors as in fig. 2) and on the two-time correlation functions $\langle \hat{P}^{\dagger}_{s+}(u)\hat{P}^{\dagger}_{i+}(v)\rangle$ and $\langle \hat{P}^{\dagger}_{s-}(u)\hat{P}^{\dagger}_{i-}(v)\rangle$. Equation (2) links $P^{\dagger}_{s\sigma} \leftrightarrow P_{i\sigma}$ and $P^{\dagger}_{i\bar{\sigma}} \leftrightarrow P_{s\sigma}$ so that the nonzero elements of the density matrix in our configuration are six:

$$\rho_{++,++} = \rho_{--,--},$$
$$\rho_{+-,+-} = \rho_{-+,-+}, \qquad (5)$$
$$\rho_{++,--} = \rho^{*}_{--,++}.$$

---

[1]Within the Lax approach [26], time-dependent noise operators have quantum statistics microscopically calculated from a nonequilibrium quantum dissipation-fluctuation theorem with respect to a Markovian environment. As instance, specialized to our system, we have that $\langle \mathcal{F}_{P^{\dagger}_{\mathbf{k}}}(u)\mathcal{F}_{P_{\mathbf{k}}}(v)\rangle = \delta(u-v)\sum_{\mathbf{k}'} W_{\mathbf{k},\mathbf{k}'}\langle \hat{P}^{\dagger}_{\mathbf{k}'}\hat{P}_{\mathbf{k}'}\rangle(u)$, where $W_{k,\mathbf{k}'}$ are Markovian scattering rates (see ref. [15] for further details on polariton systems).

[2]Formally, the EOF is defined as the minimum average pure state entanglement over all possible pure state decompositions of the mixed density matrix. It gives basically the minimum entanglement needed to construct the density matrix out of some pure states.
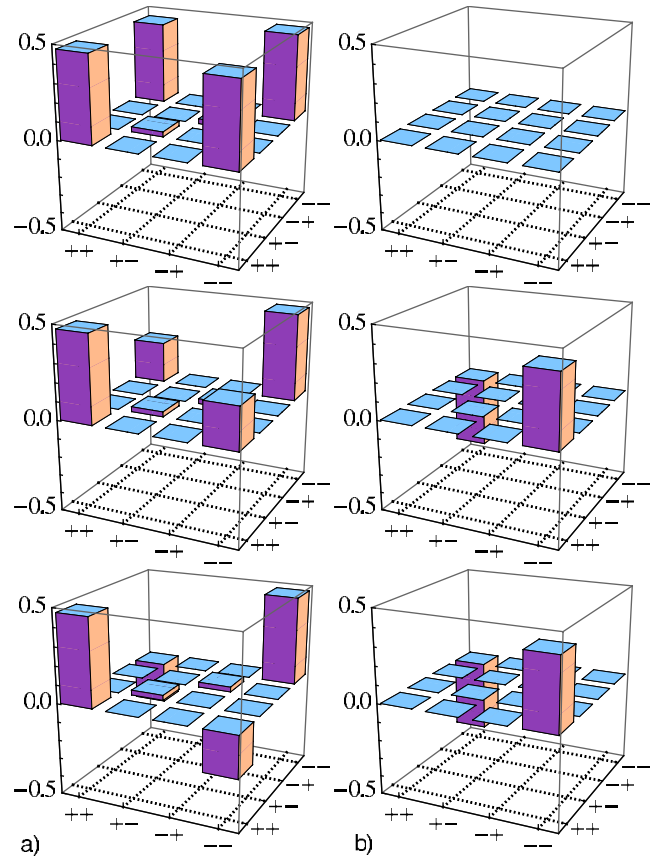

Fig. 3: (Color online) a) b) Real (imaginary) part of the density matrix in the tomographic reconstruction according to eq. (1) in the linearly cross-polarized pump configuration and for different pump polarizations in the xy-plane. The first line refers to $\hat{x}$-polarized ($\theta = 0$), the second line to $\theta = \pi/12$, the third to $\theta = \pi/6$. We point out the different phase relations appearing in the nondiagonal terms directly related to the choice of pump polarization. In the absence of longitudinal-transverse splitting [23] the system is isotropic in the polarization plane, polariton entanglement is independent of the direction of the linear pump polarization angle θ. Indeed the three cases share the same value of entanglement $E(\boldsymbol{\rho}) \simeq 0.7523$.

We integrate the system of equations, eq. (2), coupled with the underlying nonequilibrium equations for the noise correlation functions (through time-dependent fluctuation-dissipation relations) [15,26]. For a generic polarization θ, the populations are independent of θ, $N_{s/i+} = N_{s/i-}$, whereas correlations satisfy $\langle \hat{P}^{\dagger}_{s+}(u)\hat{P}^{\dagger}_{i+}(v)\rangle = -e^{i\,4\theta}\langle \hat{P}^{\dagger}_{s-}(u)\hat{P}^{\dagger}_{i-}(v)\rangle$. In fig. 3 a tomographic reconstruction is shown. We point out that different phase relations appearing in the nondiagonal terms of a reconstructed density matrix are directly related to the choice of pump linear polarization θ (see caption of fig. 3). In the absence of longitudinal-transverse splitting [23] polariton entanglement is independent of the angle of the linear pump polarization θ. As fig. 4 shows, there is a non-negligible region of the parameter space where, even in a realistic situation, high entanglement
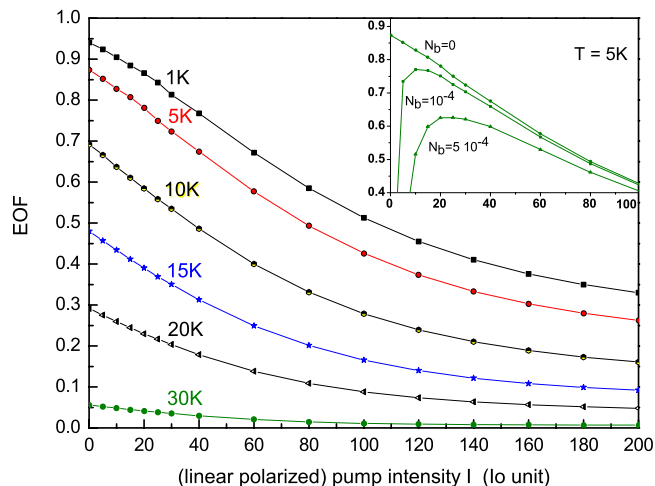
Fig. 4: (Color online) Dependence of the EOF on pumping intensity. The laser intensity I is measured in units of $I_0 = 21 \, \mathrm{photons} \, \mu\mathrm{m}^{-2}/\mathrm{pulse}$ according to ref. [9].
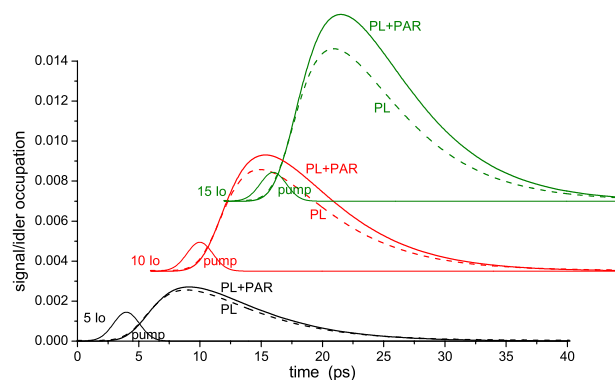

Fig. 5: (Color online) Signal/idler occupations (dashed lines: PL only; full lines: PL + parametric) vs. time for three excitation densities ($I = 5I_0$, $I = 10I_0$ and $I = 15I_0$) for $T = 5 \, \mathrm{K}$ are shown. The shape of the pump pulse is depicted for reference.

values are obtained. For increasing pump, EOF decays towards zero. This is a known consequence of the relative increase of signal and idler populations [10,11] —dominating the diagonal elements of $\hat{\rho}$— with respect to two-body correlations responsible for the nondiagonal parts, which our microscopic calculation is able to reproduce. We expect entanglement to be unaffected by both intensity and phase fluctuations of the pump laser. The former are negligible according to fig. 3, while the latter only acts on the overall quantum phase of the signal-idler pair state. Different entanglement measures generally result in quantitatively different results for a given mixed state. However, they all provide upper bounds for the distillable entanglement [2], i.e. the rate at which mixed states can be converted into the "gold standard" singlet state. Small EOF means that a heavily resource-demanding distillation process is needed for any practical purpose. Figure 4 shows how a relative small change in the lattice temperature has a sizeable impact on entanglement. As an example, for the pump intensity $I = 15I_0$, increasing the temperature from $T = 1 \, \mathrm{K}$ to $T = 20 \, \mathrm{K}$ means to corrupt the state from $E(\hat{\rho}) \simeq 0.88$ to $E(\hat{\rho}) \simeq 0.24$, whose distillation is nearly four times more demanding. For a fixed pump intensity, fig. 4 shows that, above a finite-temperature threshold, the EOF vanishes independently of the pump intensity, i.e. the influence of the environment is so strong that quantum correlation cannot be kept anymore. In physical terms, at about $30 \, \mathrm{K}$ the average phonon energy becomes comparable to the signal-pump and idler-pump energy differences, and the thermal production of signal-idler pairs is activated.

Semiconductors heterostructures are complex systems in which other noise sources are expected. The simplest way to model this additional noise is via the introduction of a constant, temperature- and pump-independent, noise background N_b. This quantity also accounts for

the noise background characterizing the photodetection system. In the inset of fig. 4, the dependence of the EOF on N_b is highlighted. In our simulation, the quantity N_b causes EOF to vanish in the limit of low pump intensity. A value of N_b of about 10^{-4} is realistic, as suggested by experiments [13] showing that it is considerably smaller than the PL-noise studied here. From inspection of the density matrix (in the $(++, +-, -+, -)$ circular-polarization basis), for pump intensity $I \to 0$, if the correlation dominates, we have as limiting case a triplet pure state

$$\rho \to \frac{1}{2} \begin{pmatrix} 1 & 0 & 0 & 1 \\ 0 & 0 & 0 & 0 \\ 0 & 0 & 0 & 0 \\ 1 & 0 & 0 & 1 \end{pmatrix}.$$

On the other hand, if the population dominates, the state becomes separable $\rho \to \frac{1}{4} \mathbb{I}$. At leading order in I, the two contributions are comparable, and $1 - E(\hat{\rho})$ is determined solely by the ratio between incoherent and parametric scattering rates. However, for ultrafast pulsed excitations, necessary for QIC applications, things are more complex and this simplified analysis fails. Indeed, the dynamical interplay between noise and parametric processes is the principal ingredient of interest and physical explanations with quantitative predicting character need to take it properly into account. For nonzero N_b, instead, the leading term in the population is constant. This explain the behaviour of EOF as $I \to 0$. Mathematically speaking, for any finite value of N_b, we have a separable state in the limit $I \to 0$. As seen in the inset of fig. 4, a finite N_b affects only the range of very low pump intensity I. Figure 5 displays the time-resolved signal/idler occupations calculated at $T = 5 \, \mathrm{K}$ for three different excitation densities. The dashed lines describe the PL contributions to the occupation. The figure clearly shows that at low excitation density the detected intensity in the signal/idler channels arises mainly from PL. Nevertheless the obtained EOF for these intensities is very high, contrarily to intuition,

but in agreement with recent results [11]. This result puts forward the robustness of pair correlations and entanglement that can be evidenced, even when noise is the dominant contribution to one-body properties.

Conclusions. – In conclusion we have shown that microcavity polaritons can be cast in an entangled state in a controlled way and we have given a ready-to-use realistic experimental configuration able to measure the EOF out of a dominant time-dependent noise background, without any need for post-processing. We point out that the outcome of a polariton parametric scattering is an *entangled state of a hybrid quasiparticle, half light and half electronic excitation, of the semiconductor* —the polariton pair— contrarily to parametric downconversion in a nonlinear crystal [6], where only the outgoing photons are entangled. Here, the emitted photons serve merely as a probe of the internal degree of entanglement. Thanks to their photon component, polaritons can sustain quantum correlations over mesoscopic distances *inside* the semiconductor. This is why they bear a unique potential as a controllable embedded mechanism to generate quantum information in a device and transfer it to localized qubits (*e.g.* spin qubits) over distances of microns [5].

$$* * *$$

REFERENCES

[1] Nielsen M. A. and Chuang I. L., *Quantum Computation and Quantum Information* (Cambridge University Press, Cambridge) 2000.

[2] Amico L., Fazio R., Osterloh A. and Vedral V., *Rev. Mod. Phys.*, **80** (2008) 517; Plenio M. B. and Virmani S., *Quantum Inf. Comput.*, **7** (2007) 1.

[3] DiVincenzo D. P., *Science*, **270** (1995) 255.

[4] Savona V., Piermarocchi C., Quattropani A., Schwendimann P. and Tassone F., *Phase Trans.*, **86** (1999) 169; Kavokin A. and Malpuech G., *Cavity Polaritons* (Elsevier, Amsterdam) 2003; Khitrova G., Gibbs H. M., Jahnke F., Kira M. and Koch S. W., *Rev. Mod. Phys.*, **71** (1999) 1591.

[5] Quinteiro G. F., Fernández-Rossier J. and Piermarocchi C., *Phys. Rev. Lett.*, **97** (2006) 097401.

[6] Mandel L., *Rev. Mod. Phys.*, **71** (1999) S274.

[7] Ciuti C., *Phys. Rev. B*, **69** (2004) 245304.

[8] Ciuti C., Schwendimann P. and Quattropani A., *Phys. Rev. B*, **63** (2001) 041303(R).

[9] Langbein W., *Phys. Rev. B*, **70** (2004) 205301.

[10] Edamatsu K., Oohata G., Shimizu R. and Ito T., *Nature*, **431** (2004) 167.

[11] Oohata G., Shimizu R. and Edamatsu K., *Phys. Rev. Lett.*, **98** (2007) 140503.

[12] Portolan S., Di Stefano O., Savasta S., Rossi F. and Girlanda R., *Phys. Rev. A*, **73** (2006) 020101(R); Glauber R. J., *Phys. Rev.*, **130** (1963) 2529.

[13] Savasta S., Di Stefano O., Savona V. and Langbein W., *Phys. Rev. Lett.*, **94** (2005) 246401.

[14] Pan J. W., Simon C., Brukner C. and Zeilinger A., *Nature*, **410** (2001) 1067.

[15] Portolan S., Di Stefano O., Savasta S., Rossi F. and Girlanda R., *Phys. Rev. B*, **77** (2008) 035433; 195305.

[16] White A. G., James D. F. V., Eberhard P. H. and Kwiat P. G., *Phys. Rev. Lett.*, **83** (1999) 3103; James D. F. V., Kwiat P. G., Munro W. J. and White A. G., *Phys. Rev. A*, **64** (2001) 052312.

[17] Bennett C. H., DiVincenzo D. P., Smolin J. A. and Wootters W. K., *Phys. Rev. A*, **54** (1996) 3824.

[18] Hill S. and Wootters W. K., *Phys. Rev. Lett.*, **78** (1997) 5022; Wootters W. K., *Phys. Rev. Lett.*, **80** (1998) 2245.

[19] Östreich Th., Schönhammer K. and Sham L. J., *Phys. Rev. Lett.*, **74** (1995) 4698; *Phys. Rev. B*, **58** (1998) 12920.

[20] Savasta S., Martino G. and Girlanda R., *Solid State Commun.*, **111** (1999) 495; Oka H. and Ishihara H., *Phys. Rev. Lett.*, **100** (2008) 170505.

[21] Schumacher S., Kwong N. H. and Binder R., *Phys. Rev. B*, **76** (2007) 245324; Savasta S. and Girlanda R., *Phys. Rev. Lett.*, **77** (1996) 4736; Savasta S., Di Stefano O. and Girlanda R., *Phys. Rev. B*, **64** (2001) 073306; *Semicond. Sci. Technol.*, **18** (2003) S294.

[22] Houdré R., Weisbuch C., Stanley R. P., Oesterle U. and Ilegems M., *Phys. Rev. B*, **61** (2000) R13333; Gurioli M., Bogani F., Wiersma D. S., Roussignol Ph., Cassabois G., Khitrova G. and Gibbs H., *Phys. Rev. B*, **64** (2001) 165309; Langbein W. and Hvam J. M., *Phys. Rev. Lett.*, **88** (2002) 047401.

[23] Kavokin K. V., Shelykh I. A., Kavokin A. V., Malpuech G. and Bigenwald P., *Phys. Rev. Lett.*, **92** (2004) 017401.

[24] Tassone F., Piermarocchi C., Savona V., Quattropani A. and Schwendimann P., *Phys. Rev. B*, **56** (1997) 7554.

[25] Ciuti C., Schwendimann P., Deveaud B. and Quattropani A., *Phys. Rev. B*, **62** (2000) R4825.

[26] Lax M., *Phys. Rev.*, **145** (1966) 110.

[27] Karr J. Ph., Baas A., Houdré R. and Giacobino E., *Phys. Rev. A*, **69** (2004) 031802(R).

[28] See, *e.g.*, Mandel L. and Wolf E., *Optical Coherence and Quantum Optics* (Cambridge University Press) 1995.

[29] See, *e.g.*, Zinn-Justin J., *Quantum Field Theory and Critical Phenomena* (Oxford Science Publications) 2002.